Contemporary Mathematics

Toral band Fatou components for the Weierstrass $\wp$ function

Jane Hawkins and Lorelei Koss

Abstract. We study the existence of unbounded Fatou components for the iterated Weierstrass $\wp$ function and discuss its dependence on lattice shapes. We show that there are open regions in shape space for lattices in $\mathbb{C}$ for which scalings of the lattice (real and complex) yield unbounded toral band Fatou components.

1. Preliminary discussion

An elliptic function is a doubly periodic meromorphic function in $\mathbb{C}$ with a period lattice Λ. The dynamics of iterated elliptic functions fit into the broader landscape of complex dynamics of meromorphic functions, worked on by many e.g., [**1, 2, 4, 6, 7, 21, 23**]. These studies have led to an interesting array of fractal Julia sets for elliptic functions (see for example [**9**] –[**15**] and [**17**] –[**20**]). In this paper we study one of the two basic building blocks of elliptic functions, the Weierstrass $\wp$ function, denoted $\wp$. The other basic function is its derivative $\wp'$, as every elliptic function with period lattice Λ can be written as a rational expression of $\wp_\Lambda$ and $\wp'_\Lambda$. The function $\wp_\Lambda$ is an even elliptic function of order 2.

There are two main points discussed in this paper; neither has been addressed in the literature before. It is well known from the references above that the Julia and Fatou sets depend on the lattice, and not only the lattice shape (such as a square or a rectangle), but also the side length. Here we look at the shape more closely; we give results to show that the more horizontal or vertical looking lattices allow for a wider variety of Julia sets and Fatou components, while the more regular shapes like square and rhombus shapes whose short diagonals are still longer than a side of the rhombus, have less variety.

Our discussion adds another variable that seems to affect the dynamics, which is, how the lattice is situated relative to the real and imaginary axes. For example, horizontally situated lattices seem to have a wider variety of vertical Fatou components than vertically placed ones (defined below). While lattices give rise to many different fundamental regions or period parallelograms, (see Figure 1), some definitely appear to be more horizontal, others more vertical, and others look more blockish. For elliptic functions, the Julia sets are doubly periodic, so while we do not expect unbounded Fatou components for $\wp_\Lambda$, and they cannot occur for square

2010 *Mathematics Subject Classification.* Primary 37F10, 37F12, 30D05.

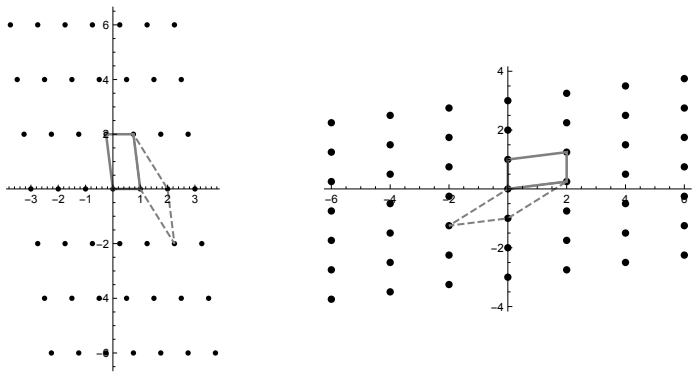

FIGURE 1. The lattice Λ on the left appears to be more vertical than the one on the right, which is $i\Lambda$. This can be seen by drawing a few period parallelograms.

and triangular lattices, they occur more frequently than first thought when changing both the lattice shape and its orientation. These together yield many types of Fatou and Julia sets even when just looking at the single function $\wp$. Moreover, the occurrence of toral bands, once thought to be rare in parameter space, is now established to be very common, occurring in open sets of shapes.

1.1. Background notation and results. Lattices determine double periods for elliptic functions. By $\Lambda = [\lambda_1, \lambda_2]$ we denote the group

$$\Lambda = \{m\lambda_1 + n\lambda_2 \colon m, n \in \mathbb{Z}\} \subset \mathbb{C}. \tag{1.1}$$

Assuming $\lambda_1, \lambda_2 \in \mathbb{C}$ are non-zero and linearly independent over $\mathbb{R}$, we call Λ a *lattice*. A lattice Λ acts on $\mathbb{C}$ by translation, each $\omega \in \Lambda$ inducing the transformation:

$$T_\omega : z \mapsto z + \omega.$$

We denote the coset of $\mathbb{C}/\Lambda$ containing z by $[z]$.

A closed, connected parallelogram Q is a *fundamental paralleogram* for Λ if

(1) for each $z \in \mathbb{C}$, Q contains at least one point in the same Λ-orbit as z;
(2) no two points in the interior of Q are in the same Λ-orbit.

In this paper we focus on parallelograms, but other regions are possible for Q that satisfy (1) and (2). A *real lattice* Λ is one such that $\overline{\Lambda} = \Lambda$, where $\overline{z}$ denotes complex conjugation and $\overline{\Lambda} = \{\overline{\lambda} : \lambda \in \Lambda\}$.

For a general elliptic function over Λ, denoted f_Λ (or f), z_0 is a critical point if $f'_\Lambda(z_0) = 0$ and $f_\Lambda(z_0)$ is a critical value. The *Fatou set* $F(f)$ is the set of points $z \in \mathbb{C}_\infty$ such that $\{f^k \colon k \in \mathbb{N}\}$ is defined and normal in some neighborhood of z. The *Julia set* $J(f)$ is the complement of the Fatou set on the sphere. For each lattice Λ, every elliptic function with period lattice Λ is of Class S [**4**] and does not have wandering domains [**2**] or Baker domains [**23**]. We summarize the types of Fatou components that can occur.

THEOREM 1.1. *If f_Λ is an elliptic function with period lattice Λ, then every component of $F(f_\Lambda)$ is preperiodic, and each forward invariant Fatou component contains one of the following:*

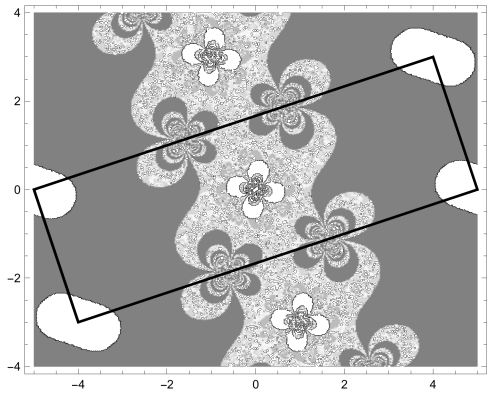

FIGURE 2. This shows a toral band for $\wp_\Xi$ with a rectangular lattice $\Xi = k[1, 3i]$, and $k = 1 + 3i$.

(1) a linearizing neighborhood of an attracting periodic point;
(2) a Böttcher neighborhood of a superattracting periodic point;
(3) an attracting Leau petal for a periodic parabolic point. The periodic point is in $J(f_\Lambda)$;
(4) a periodic Siegel disk containing an irrationally neutral periodic point.
(5) a Herman ring.

Order 2 elliptic functions do not have Herman rings, so Theorem 1.1(5) does not occur for $\wp_\Lambda$ [**10, 22**]. We define the types of unbounded Fatou components that are possible in this setting.

DEFINITION 1.2. Assume that $f_\Lambda = f$ is an elliptic function over the lattice $\Lambda = [\lambda_1, \lambda_2]$. Then

(1) A Fatou component A_0 of f is a *toral band* if A_0 contains an open subset U which is simply connected in $\mathbb{C}$, but U projects to a topological band around the torus $\mathbb{C}/\Lambda$ containing a homotopically nontrivial curve.
(2) A toral band A_0, is a *double toral band* if it projects to a set in the torus $\mathbb{C}/\Lambda$ that contains closed paths that generate the fundamental group $\pi_1(\mathbb{C}/\Lambda)$;
(3) We say A_0 is a *vertical toral band* if there is a line $L \subset A_0$ where L is parallel to the imaginary axis; and A_0 is a *horizontal toral band* if there is a line $L \subset A_0$ where L is parallel to the real axis.
(4) If A_0 is a toral band that is not double, it is called a *single toral band*.
(5) A toral band is *nonperiodic* if it maps onto a cycle of Fatou components but is not part of the cycle.

REMARK 1.3. Not every toral band for $\wp_\Lambda$ needs to be either horizontal or vertical; a toral band is often parallel to one of the edges of a fundamental parallelogram region. For example, a rectangular lattice scaled by a complex number is still rectangular, but its sides are not parallel to any axis, as shown in Figure 2.

The *Weierstrass elliptic function* is defined for each $z \in \mathbb{C}$, by

$$\wp_\Lambda(z) = \frac{1}{z^2} + \sum_{\lambda \in \Lambda \setminus \{0\}} \left(\frac{1}{(z-\lambda)^2} - \frac{1}{\lambda^2} \right). \tag{1.2}$$

The map $\wp_\Lambda$ is an even elliptic function with poles of order 2 at lattice points. The derivative $\wp'$ is an odd elliptic function of order 3, also periodic with respect to Λ, and obtained by term by term differentiation of (1.2).

Using the notation from (1.1), we define $c_1 = \lambda_1/2$, $c_2 = \lambda_2/2$, and $c_3 = \lambda_1/2+\lambda_2/2$ to denote the half lattice points in a fundamental parallelogram Q. This is sometimes ambiguous since generators can change; however the critical points of $\wp_\Lambda$ are $[c_j]$ for $j = 1, 2, 3$. The critical values of $\wp_\Lambda$ are denoted by $e_j = \wp_\Lambda(c_j)$ for $j = 1, 2, 3$. They are distinct for each lattice, and they satisfy the relationship

$$e_1 + e_2 + e_3 = 0, \quad e_1e_3 + e_2e_3 + e_1e_2 = \frac{-g_2}{4}, \quad e_1e_2e_3 = \frac{g_3}{4}, \tag{1.3}$$

we define g_2 and g_3 as follows. Given a lattice Λ, define

$$S_n = \sum_{\lambda\in\Lambda,\lambda\neq 0} \lambda^{-n}, \tag{1.4}$$

which converges absolutely for all $n \geq 3$. We then set

$$g_2 = 60\, S_4, \text{ and } \mathrm{g}_3 = 140\, \mathrm{S}_6,$$

so that $\wp'(z)^2 = 4\wp_\Lambda(z)^3 - g_2\wp_\Lambda(z) - g_3$. Let $\triangle = g_2^3 - 27g_3^2$ denote the discriminant of the cubic polynomial $p(x) = 4x^3 - g_2z - g_3$, which satisfies $\triangle \neq 0$ since the e_js are distinct.

2. Toral bands for $\wp_\Lambda$ real and nonreal lattices

A goal of this paper is to show that there are many toral bands occurring in $F(\wp_\Lambda)$ for an open set of lattices in shape space (see Figure 7). Earlier papers ruled out toral bands for the square and triangular shapes, [**11, 5**], each of which is represented by a single point in shape space. We also argue, with some supporting results, that because of the shape of the primary region for τ space, most of the time if we use constants k that are purely imaginary, then we see more vertical toral bands. The presence of toral bands impacts the geometry of the complementary Julia set, as shown below by comparing the Julia sets in Figures 2, 4 - 6, 8, and 10. Up to now, most toral bands have come from more elaborate constructions of elliptic functions, though an early paper by the authors [**11**] provided examples of toral bands for $\wp_\Lambda$.

THEOREM 2.1. [**10**] *For a lattice $\Lambda = [\lambda_1, \lambda_2]$ the following hold for every even elliptic function $f_\Lambda = f$ with period lattice Λ:*

1. *$(-1)J(f) = J(f)$ and $(-1)F(f) = F(f)$.*
2. *There is symmetry of $F(f)$ and $J(f)$ about each half lattice point; i.e., for any $j = 1, 2, 3$,*

$$f(c_j + tc_k) = f(c_j - tc_k), \text{ and } f(c_j + z) = f(c_j - z) \tag{2.1}$$

for $t \in \mathbb{R}, z \in \mathbb{C}$.

COROLLARY 1. *For a real lattice Λ*

1. *$F(\wp_\Lambda)$ and $J(\wp_\Lambda)$ are symmetric about all half lattice lines parallel to the axes and about all critical points.*
2. *$\overline{F(\wp_\Lambda)} = F(\wp_\Lambda)$ and $\overline{J(\wp_\Lambda)} = J(\wp_\Lambda)$*

PROPOSITION 1. *If $\wp_\Lambda$ has a toral band $T \subset F(\wp_\Lambda)$, then T is the only toral band on $\mathbb{C}/\Lambda$ and $\wp_\Lambda$ maps T (in $\mathbb{C}$) either to itself or into a bounded component of $F(\wp_\Lambda)$. In particular, if $T_1 \neq T_2$ are disjoint toral bands in $F(\wp_\Lambda) \subset \mathbb{C}$, then $T_2 = T_1 + \lambda$ for some $\lambda \in \Lambda$ and T is a single toral band.*

PROOF. The authors showed in ([**13**],Theorem 2.15) that a toral band must contain at least 2 residue classes of critical points. There are only 3 residue classes of critical points for $\wp_\Lambda$, so at most one toral band can occur. Suppose there are two disjoint toral bands in $\mathbb{C}$, say T_1 and T_2. Then they must project to the same set on $\mathbb{C}/\Lambda$ by the first result. Therefore $T_2 = T_1 + \lambda$ for some $\lambda \in \Lambda$. □

REMARK 2.2.
(1) Following from the definitions, every vertical toral band must intersect $\mathbb{R}$ and every horizontal toral band intersects the imaginary axis. In fact every toral band that is not horizontal must intersect $\mathbb{R}$.
(2) We know from double periodicity that toral bands cannot themselves be Siegel disks or Herman rings (see [**13**]). However, there are elliptic functions f with a toral band T for which $f(T)$ is a Siegel disk [**13**].
(3) Multiple toral bands are possible, and exist, for higher order elliptic functions [**13**].

We showed in earlier papers [**9**] –[**15**] that real and complex scalings of lattices Λ along the imaginary axis and vertical boundary of the primitive fundamental lattice region shown in Figure 1 give rise to many toral bands for $\wp_\Lambda$. We expand the result to include large regions of lattice shapes in the region in Figure 7. We start with the following proposition, using a function, from [**8**].

DEFINITION 2.3. For a lattice generated by $[1, \tau]$, we define

$$I(\tau) = \frac{g_2^3}{27 g_3^2}(\tau).$$

THEOREM 2.4. *$I(\tau)$ is meromorphic in the open upper half plane, with poles at zeroes of $g_3(\tau)$. There is a double pole at $\tau = i$, a zero of $I(\tau)$ occurs at $\tau = \exp(2\pi i/3)$, and $I(\tau) < 0$ for all τ with $|\tau| = 1$ and $\arg(\tau) \in (2\pi/3, \pi/2)$. Every negative real number is $I(\tau)$ for some τ on that arc.*

A version of this can be found in ([**8**], Thm 3.4).

PROPOSITION 2. *Let $\mathfrak{U}$ denote the primitive region for lattice shape space, defined by $\tau \in \mathbb{C}$ satisfying*

$$\mathrm{Im}(\tau) > 0, -1/2 \leq \mathrm{Re}(\tau) < 1/2, |\tau| \geq 1, \text{ and } |\tau| > 1 \text{ if } \mathrm{Re}(\tau) > 0.$$

Then the following hold for $\Lambda = [1, \tau]$:

(1) $g_2(\tau), g_3(\tau)$, and $J(\tau) = I/(I-1)(\tau) = g_2^3/\Delta$ are $\mathbb{Z}$ periodic and analytic on $\mathfrak{U}$; that is, their values are unchanged under the map $T(\tau) = \tau + 1$;
(2) As $\mathrm{Im}(\tau) \to \infty$ in $\mathfrak{U}$, $\mathrm{Arg}(\tau) \to \pi/2$, and $g_2 \to 120\zeta(4) = 4\pi^4/3 = g_2^*$, where ζ is the Riemann zeta function given by

$$\zeta(s) = \sum_{r=1}^{\infty} r^{-s}, s > 1.$$

We also have that $\lim_{\mathrm{Im}(\tau)\to\infty} g_3 = g_3^*$ exists and the limits satisfy

$$(g_2^*)^3 = 27(g_3^*)^2.$$

(3) *The doubly periodic function $\wp_{[1,\tau]}$ converges to a simply periodic function, with period 1, and the critical values converge to $e^* = \sqrt{g_2^*/3}$, $-1/2e^*$, and $-1/2e^*$.*
(4) *If the lattice is generated by $[k, k\tau]$, then $e^*(k\tau) = k^{-2}e^*$.*

Remarks about the proof. Most of these are classical results and can be found in sources like [**8**] and [**16**]. Fixing $|\tau| = b$, in order for $\tau \in \mathfrak{U}$, we must have $\arg(\tau) \in (\arccos(-1/2b), \arccos(1/2b))$. Clearly as $\tau \to \infty$ in $\mathfrak{U}$, $\arg(\tau) \to \pi/2$ and $\mathrm{Re}(\tau)$ remains bounded; therefore $\mathrm{Im}(\tau) \to \infty$ and the lattice approaches a degenerate one-dimensional lattice generated by a single generator [1]. This is because the lattice points along the integers remain unchanged while all other lattice points "disappear" to ∞. Using ([**8**], Theorem 1.2), it follows that the sums S_n defined in (1.4), converge to $2\,\zeta(n)$ for even positive integers n, and recall that $g_2 = 60S_4$ and $g_3 = 140S_6$. □

Algorithm for obtaining vertical toral bands for $\wp_\Lambda$.

This method yields toral bands that are forward invariant or periodic.

(1) We start by choosing a lattice shape $\Lambda = [1, \tau]$, with $\tau \in \mathfrak{U}$. Labelling $e_1 = \wp_\Lambda(1/2)$, and $e_2 = \wp_\Lambda(\tau/2)$ and $e_3 = -e_1 - e_2$, we choose τ large enough so that e_1 is close to its limiting value, $(2/3)\pi^2 \approx 6.5797$. (Note: $|\tau| = 2$ seems to be big enough for this, but it is likely necessary for it to be larger in the algorithm below.) Once $|\tau|$ is large enough, any choice of τ works.
(2) By multiplying $[1, \tau]$ by i, we replace the lattice Λ by $\Xi = [i, \tau i]$, whose shortest generator lies on the imaginary axis. We (re)label the critical points so that $c_2 = i/2, c_1 = i\tau/2$, and $c_3 = c_1 + c_2$. We label the critical values accordingly.
(3) We next scale with a real number to be close to attracting fixed points, so we use a small variation on the result from [**11**] to choose $\kappa_0 = \sqrt[3]{e_1} \approx 1.75$. This value can be better pinpointed: we have $e_1 \approx -e_2/2$, and e_2 is negative and not far from $-e^* \approx -6.5797$. This pushes e_3 close to e_1 as well. These critical values are, in general, complex numbers with small imaginary part, so the value varies a little and becomes much more accurate as τ increases in $\mathfrak{U}$. The exact value, $\kappa = \sqrt[3]{2e_1/i\tau}$ yields a superattracting fixed point for the resulting $\wp_{\kappa\Lambda}$ whose basin contains $\kappa^{-2}e_1$ as well as the associated critical point $c_1^{(\kappa)} = i\kappa\tau/2$. The fixed point is near $c_1^{(\kappa)}$, and its immediate basin of attraction contains both $\kappa^{-2}e_1$ and $\kappa^{-2}e_3$, which are now a lot closer to each other. Therefore a preimage of e_3 is in the basin as well, so we have a fixed toral band containing two critical points and two critical values. Often a value near $\kappa = 1.75$ works well, though the value depends on e_3.
(4) The resulting lattice, $\kappa\Xi = i\kappa[1, \tau]$, now has a vertical toral band since the images of the critical points $c_1^{(\kappa)}$ and $c_3^{(\kappa)}$ are in the same Fatou component. The critical points $c_1^{(\kappa)}$ and $c_3^{(\kappa)}$ have the same real part, namely $\mathrm{Re}(i\tau)/2$, so are parallel to the imaginary axis.
(5) As κ moves around in $\mathfrak{U}$ period doubling bifurcations occur while the toral band remains. The bifurcation values depend on τ.

Algorithm for obtaining horizontal toral bands for $\wp_{k\Lambda}$.

This method yields toral bands that are nonperiodic.

(1) We start with a lattice $\Lambda = [1, \tau]$, choosing $\tau \in \mathfrak{U}$. We label $e_1 = \wp_\Lambda(1/2)$, and $e_2 = \wp_\Lambda(\tau/2)$ and $e_3 = -e_1 - e_2$ and choose τ large enough so that e_1 is close to its limiting value, $(2/3)\pi^2 \approx 6.5797$ as above. (Note: $|\tau| = 3$ seems to be big enough for this, and could be smaller.)
(2) We next adjust to be close to attracting fixed points (and higher period attracting orbits), so we use a result from [**11**] to choose $k_0 = \sqrt[3]{2e_1} \approx 2.36$; this value yields a superattracting fixed point for the resulting $\wp_{k\Lambda}$ whose basin contains $k^{-2}e_1$ and kc_1, but the immediate basin of attraction needs to be a bit bigger so that one of its preimages can contain both $k^{-2}e_2$ and $k^{-2}e_3$, which are now a lot closer to each other. Often a value near $k = 2.4$ works well.
(3) The resulting lattice, $k\Lambda = k[1, \tau]$, now has a horizontal toral band containing representatives from the critical point classes $[kc_2]$ and $[kc_3]$, since the images of the critical points kc_2 and kc_3 are in the same Fatou component. The critical points kc_2 and kc_3 have the same imaginary part, namely $\mathrm{Re}(\tau)/2$, so are parallel to the real axis and the toral band is horizontal.
(4) We note that the number of iterations before the points $\wp^j_{k\Lambda}(kc_2)$ and $\wp^j_{k\Lambda}(kc_3)$ land in the immediate attracting basin containing the fixed point can vary.
(5) As k increases (very slowly in $\mathbb{R}$), period doubling bifurcations occur while the toral band remains.

If $|\tau|$ is large enough (bigger than 2), most of the k spaces look very similar to the space in Figure 3, where the white region shows the values of k for which $\wp_{k\Lambda}$ has a toral band. We have just outlined the proof of the following.

THEOREM 2.5. *There exists an $\alpha > 1$ such that for any $|\tau| > \alpha$, the lattice $\Lambda = [1, \tau]$ can be scaled by real or imaginary complex numbers so that $\wp_{k\Lambda}$ has either a vertical or a horizontal toral band.*

There are reductions possible in every k space, and a typical k-space is shown in Figure 3, with 6-fold symmetry apparent; results on this appear in [**11**].

REMARK 2.6. We summarize the properties of the toral bands that the algorithms produce for the Weierstrass elliptic $\wp$ function. Suppose a lattice $\Lambda = k[1, \tau]$, $\tau \in \mathfrak{U}$, with k chosen using one of the algorithms, has a toral band in $F(\wp_{k\Lambda})$.

(1) The discriminant function $\triangle = g_2^3 - 27g_3^2 \neq 0$ is small, which is equivalent to saying that the function $I(\tau) = \dfrac{g_2^3}{27g_3^2}(\tau)$, is very close to 1. However the rates at which $I(\tau)$ and $\triangle(\tau)$ approach their limits as τ increases varies, as discussed in (5) below; $I(\tau)$ approaches 1 earlier (than $\triangle$ shrinks) and gives toral bands.
(2) If k is either purely imaginary or real, then the toral band is vertical or horizontal, respectively.
(3) Since the existence of a toral band is stable when an attracting orbit exists for $\wp_{k_o\Lambda}$, then there exists a neighborhood of k_o such that for k in the neighborhood, the toral bands will persist, but will no longer be vertical

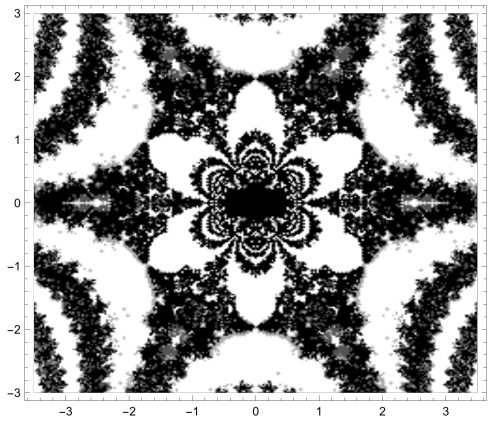

FIGURE 3. Starting with the lattice $\Lambda = [1, 3i]$, we show k-space, where points that are white have multiple critical points attracted to periodic orbits. This is used to study the properties of $\wp_{k\Lambda}$ for each complex number k shown.

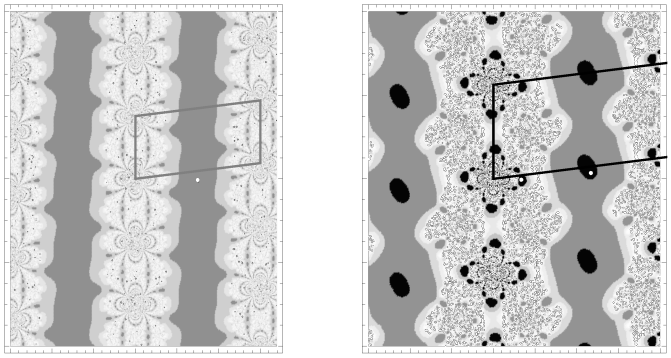

FIGURE 4. Starting with the lattice $\Lambda = [1, -.25 + 2i]$, we scale it by $k = 1.5i$ and the left and $k = 2.25i$ shown in Figure 3; on the left an attracting fixed point is marked, and on the right, and attracting period 2 orbit, both are white.

or horizontal. Instead, $F(\wp_{k\Lambda})$ will contain lines parallel to a side of the resulting period parallogram for $k\Lambda$.

(4) The labelling convention described above uses $c_1 = 1/2$ or $i\tau/2$ to denote the critical point closest to the positive real axis, $c_2 = \tau$ or $i/2$ for the critical point closest to the positive imaginary axis, and $c_3 = c_1 + c_2$. Then for the scaled lattice $[k, k\tau]$, the toral bands constructed above always contain either kc_1 and kc_3, or kc_2 and kc_3. In the first instance the toral band is vertical and in the second instance it is horizontal. The main point is that for the scaled critical values, $e_3^{(k)}$ is extremely close to either $e_1^{(k)}$ or $e_2^{(k)}$ in each case.

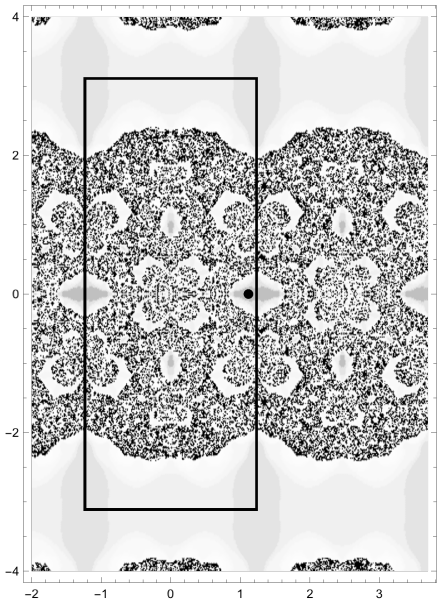

FIGURE 5. Starting with the rectangular lattice $\Lambda = [1, 2.52i]$, we scale by $k = 2.47$ and see that horizontal toral bands appear. They also have a period doubling cascade as k increases, as a small Mandelbrot set appears. in k-space for this lattice.

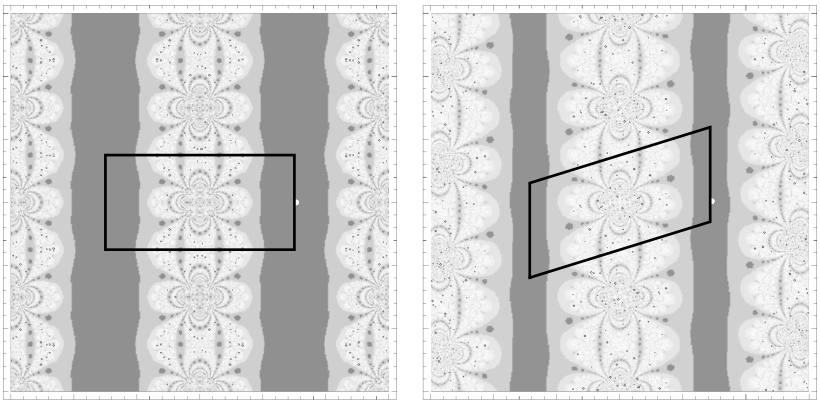

FIGURE 6. Starting with the rectangular lattice $\Lambda = [1, \tau]$, with $\tau = 2i$ on the left and $\tau' = \kappa\tau$, with $\kappa = 0.955336 - 0.29552i$, a small rotation of τ by $\exp(.3i)$ in the primary region of lattice shapes, we use the same scaling factor and see that vertical toral bands persist.

(5) In the case where the critical values $e_1^{(k)}$ and $e_3^{(k)}$ lie close to each other, we set $e_1^{(k)} = \eta$ for convenience of notation to analyze the algorithm. Using Eqn (1.3), the critical values satisfy the equations $e_2^{(k)} = -2\eta - j$ and $e_3^{(k)} = \eta + j$, for some complex number j with very small modulus. Applying Eqn (1.3) again, we have $g_2 = 4(3\eta^2 + 3\eta j + j^2)$ and $g_3 = -4(2\eta^3 + 3\eta^2 j + \eta j^2)$. The discriminant gives

$$\begin{aligned}\triangle &= g_2^3 - 27g_3^2 \\ &= 1296\,\eta^4 j^2 + 2592\,\eta^3 j^3 + 1872\,\eta^2 j^4 + 576\,\eta j^5 + 64 j^6,\end{aligned}$$

which is not very close to 0 when η is a value greater than 3; even if $j = .1$, it is large. The term $1296\,\eta^4 j^2$ dominates, and gives a value above 1000 when $j = .1$. However, the function

$$I(\tau) = \frac{g_2^3}{27g_3^2}(\tau),$$

is very close to 1 when η is between 3 and 4 and $j \leq .5$ and this gives toral bands.

In the case where the critical values $e_2^{(k)}$ and $e_3^{(k)}$ lie close to each other, using the same notation, the critical values satisfy $e_2^{(k)} = -\eta/2 + j$ and $e_3^{(k)} = -\eta/2 - j$, for some complex number j with very small modulus. Eqn (1.3) gives $g_2 = 3\eta^2 + 4j^2$ and $g_3 = \eta^3 - 4\eta j^2$. The discriminant $\triangle = g_2^3 - 27g_3^2 = 324\eta^4 j^2 - 288\eta^2 j^4 + 64 j^6$ is increasing in η for fixed j. However, the function

$$\begin{aligned}I(\tau) &= \frac{g_2^3}{27g_3^2}(\tau) \\ &= \frac{(3\eta^2 + 4j^2)^3}{27(\eta^3 - 4\eta j^2)^2},\end{aligned}$$

is very close to 1 when j is reasonably small, again resulting in toral bands.

3. Failure of existence of toral bands for $\wp_\Lambda$ for certain lattice shapes

It is now well-known that every lattice shape admits scalars for which some or all of the critical points land on poles [**12**]. In this section we give arguments that toral bands are rare or possibly even nonexistent in the setting where $\Lambda = k[1, e^{i\theta}]$, with $\theta \in [\pi/2, 2\pi/3]$, for every $k \in \mathbb{C}\backslash\{0\}$. This curve of lattice shapes makes up the lower boundary of the region in Figure 7. The endpoints of the arc correspond to square and triangular lattices, and it has already been shown, in [**10, 11, 12, 5, 20**] that $F(\wp_\Lambda)$ for Λ square or triangular contains no toral bands. This is because the critical values are maximally spread out and no amount of scaling will bring two of them into the same Fatou component. In this section we address the algorithms given in the previous section, but apply them to lattices when $|\tau|$ is 1.

3.1. Medium rhombic lattices. A rhombic lattice is one where there is a period parallelogram with all four sides of the same length. A medium rhombic lattice has the additional property that the length of the shortest diagonal is longer than one of its sides. Some notable cases occur when $\tau = i$, and the lattice is square so both diagonals have the same length (longer than the side of the square), and the triangular lattice, where they are equal since the lattice is comprised of 2 equilateral

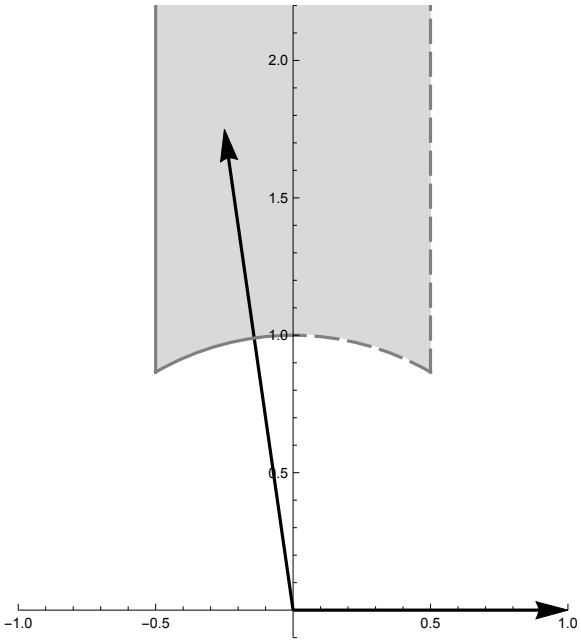

FIGURE 7. A primary region for lattices. When $|\tau| = 1$, only the lattices with generators $\Lambda = [1, e^{i\theta}]$, with $\theta \in [\pi/2, 2\pi/3]$ are needed. The endpoints of the interval give square ($\theta = \pi/2$) and triangular ($\theta = 2\pi/3$) lattices. The dashed curves are not in the region.

triangles. The other lattice shapes in this category are made by deforming a square lattice to a triangular one by increasing one angle. The next result follows from a variety of classical results given in Duval, for example.

If Λ is a real lattice and is also medium rhombic, then it can be written as $\Lambda = [a + ib, a - ib]$, $a, b \in (0, \infty)$. If $a < b$, then we say Λ is *vertical*, and otherwise it is *horizontal*, as in the first case the longer diagonal is parallel to the imaginary axis, and in the other the longer diagonal lies along the real axis.

PROPOSITION 3. *If $|\tau| = 1$, and $\tau = \exp(i\theta)$, with $\theta \in [\pi/2, 2\pi/3]$, then the following hold for $\Lambda = [1, \tau]$:*

1. *Λ is a medium rhombic lattice .*
2. *Λ is similar to a real lattice say Λ_h, which is a horizontal medium rhombic lattice.*
3. *$\Lambda_h(g_2, g_3)$ has $g_2 < 0$ and $g_3 < 0$; if $\theta \in (\pi/2, 2\pi/3)$ then $\Lambda_h = k[1, e^{i\theta}] = [a + ib, a - ib]$, where $k = ie^{-i\theta/2}$ and $a = \sin(\theta/2)$, $b = \cos(\theta/2)$.*
4. *Λ is also similar to a real lattice Λ_v, which is a vertical medium rhombic lattice.*
5. *$\Lambda_v(g_2, g_3)$ has $g_2 < 0$ and $g_3 > 0$; if $\theta \in (\pi/2, 2\pi/3)$ then $\Lambda_v = [b + ia, b - ia]$, where a and b are as above.*
6. *For Λ either Λ_h or Λ_v, if z lies on a vertical line passing through any real lattice point or any real half-lattice point, then $\wp_\Lambda(z) = (-\infty, e_3]$.*

(7) *Defining* $I(\tau) = \dfrac{g_2^3}{27g_3^2}(\tau)$, $I(\tau) < 0$ *for all* τ *with* $|\tau| = 1$, $\arg(\tau) \in (2\pi/3, \pi/2)$. *Also every negative real number is* $I(\tau)$ *for some* τ *in that arc.*

Conversely, if a real lattice $\Lambda = \Lambda(g_2, g_3)$ *has* $g_2 < 0$ *and* $g_3 < 0$, *then* Λ *is similar to a lattice with* $\Lambda = [1, \tau]$ *with* $|\tau| = 1$.

Proof. Most of these results are found in Duval [**8**]. The proof (3) and (4) follows from the homogeneity equations. □

The dynamics of $\wp_\Lambda$ change as a medium rhombic lattice Λ rotates and stretches by scalars, but some invariants are unaffected. In particular, the next result shows that scaling a medium rhombic lattice leaves the rather large angles between the e_js the same.

Proposition 4. *If* $|\tau| = 1$, *and* $\tau = \exp(i\theta)$, *with* $\theta \in [\pi/2, 2\pi/3]$, *so that* $\Lambda = [1, \tau]$ *is medium rhombic. Then using* $k = \exp(-i\theta/2)$, *we have the following:*

- $k\Lambda$ *is a real lattice so for all* $z \in \mathbb{C}$, $\overline{\wp_{k\Lambda}(z)} = \wp_{k\Lambda}(\overline{z})$.
- *Denoting* $c_1 = 1/2$, $c_2 = \tau/2$ *and* $c_3 = c_1 + c_2$ *as critical points of* $\wp_\Lambda$, *we set* r_1, r_2, *and* r_3 *as the corresponding critical points for* $k\Lambda$; *we have that* $r_3 \in \mathbb{R}$.
- *Denoting* $e_1 = \wp_\Lambda(1/2)$, $e_2 = \wp_\Lambda(\tau/2)$ *and* $e_3 = \wp_\Lambda(c_3)$ *as the three critical values of* $\wp_\Lambda$, *we set* s_1, s_2, *and* s_3 *as the corresponding critical values for* $k\Lambda$; *we have that* $s_3 \in \mathbb{R}$, *and* $s_2 = \overline{s_1}$;
- $e_1 = k^2 s_1$, $e_2 = k^2 s_2$, *so* $\arg(e_1/e_2) = \arg(s_1/s_2)$; *also* $e_2 = \exp(2\theta)\overline{e_1}$.

Proof. The statements follow from the homgeneity equations and the elementary observation that $\overline{k} = k^{-1}$. Under our hypotheses we have these identities: $\overline{k\Lambda} = k\Lambda$, both being the same real lattice, so $\overline{\wp_{k\Lambda}(kz)} = k^2\overline{\wp_\Lambda(z)}$. We note that $k\Lambda = \overline{k\Lambda}$ implies that $\Lambda = k^{-2}\overline{\Lambda}$, so we use:

$$s_2 = \overline{s_1} = \overline{(k^{-2})e_1} = k^2\overline{e_1}.$$

Also, $s_2 = k^{-2}e_2$ so the result follows. □

Failure of the algorithm when Λ is medium rhombic lattice. It is the first step in the above algorithms that fails when Λ is medium rhombic. Step 1 tells us to move through $\mathfrak{U}$ until $I(\tau)$ is quite close to 1. This is the starting point to look for attracting dynamics. However, when $|\tau| = 1$ in $\mathfrak{U}$, as we move counterclockwise with $\tau = \exp(i\theta)$, from $\theta = \pi/2$ to $\theta = 3\pi/2$, $I(\tau)$ ranges from 0 to $-\infty$, hitting all the negative real numbers along the way.

We can use the result from [**11**] to obtain infinitely many values of k for which the resulting lattice $k\Lambda$ yields a superattracting or attracting fixed point and attracting orbits of higher period, but this is not enough. Both the critical points and the critical values are too separated to allow for more than one to appear in a single Fatou component.

We conjecture that these lattices, occurring at the bottom of the primary region of lattice shapes cannot have toral bands, and we give some partial results in that direction. We start by using the result from ([**11**], Lemma 7.2) to show that given a medium rhombic lattice we can scale it by $k = \sqrt[3]{e_j/c_j}$, $j = 1, 2$ or 3, choosing the cube root so that we have a real lattice with a superattracting fixed point. For

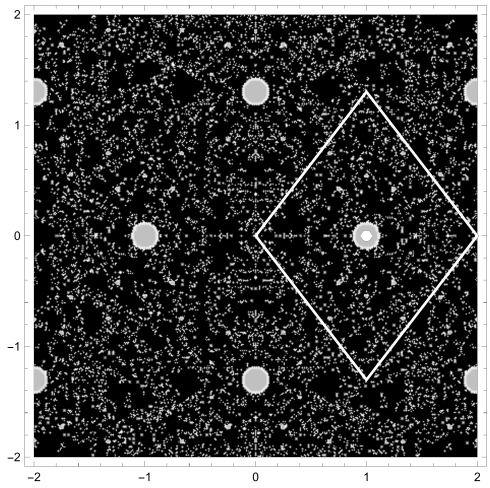

FIGURE 8. $J(\wp_\Xi)$ is quite thick, with no toral bands for a superattracting fixed point, for $\Xi = k[1, \exp(7\pi i/12)]$, a medium rhombic lattice.

large regions in τ space, this lands us near or among parameters giving toral bands, but the next example shows this does not happen in this setting.

EXAMPLE 3.1. We show a Julia and Fatou set for a medium rhombic lattice of the form $\Xi = k[1, \exp(7\pi i/12)] = k[1, \tau]$. We note that τ is halfway along the lower boundary of the region shown in Figure 7. Using ([**11**], Lemma 7.2) we obtain that for $(g_2, g_3) \approx (-19.8033, 23.7727)$ we have not changed τ but the resulting map $\wp_\Xi$ has a real superattracting fixed point. In fact the results in [**12**] show that there are infinitely many values of k with this property, and infinitely many ℓs such that $\Xi = \ell[1, \tau]$ satisfying $J(\wp_\Lambda) = \hat{\mathbb{C}}$. For these, the techniques given in [**12**] and some discussion below show that there are no toral bands.

We finish with a result in the direction of showing that we cannot have toral bands for medium rhombic lattices. While we state the lemma for one scalar, there are infinitely many that work.

PROPOSITION 5. *If $\Lambda = [1, \tau]$ has critical points for $\wp_\Lambda$ labelled by $c_1 = 1/2, c_2 = \tau/2$, and $c_3 = c_1 + c_2$, then scaling by: $k = \sqrt[3]{e_3/(2c_3)}$ gives a lattice with $e_3^{(k)} = \wp_{k\Lambda}(kc_3)$ a pole. Moreover, $\arg(k) = -\arg(\tau)/2$, so the lattice $k\Lambda$ is real, $\wp_{k\Lambda}^n(kc_j) \in \mathbb{R}$ for $n \geq 2$ and there are no toral bands.*

PROOF. Results very similar to this have been proved in [**10**] and [**20**] and the proof follows from the homogeneity equations. Since we know that $e_3^{(k)} = 2(kc_3)$, a pole, it follows that the real parts of $e_3^{(k)}$ and $e_3^{(k)}$ are critical points $(-kc_3)$. Therefore $\wp_{k\Lambda}(e_1^{(k)}) = \wp_{k\Lambda}(e_2^{(k)}) \in \mathbb{R}$, using Proposition 3, (6); hence there can be no toral bands. This is because there are no nonrepelling real cycles and the critical orbits remain on $\mathbb{R}$. □

The proof details use that the scaled lattice $k\Lambda$ is vertical rhombic, and therefore yield the result that $J(\wp_{k\Lambda}) = \hat{\mathbb{C}}$, but the techniques appear in [**10**] and [**20**] so we

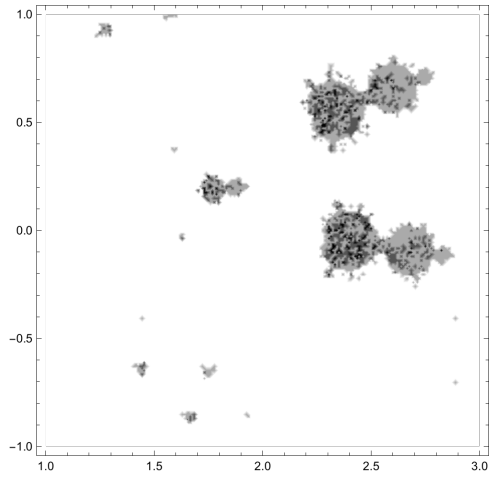

FIGURE 9. We scale the lattice $[1, \tau]$, $\tau = \exp(i\theta)$ a medium rhombic lattice, by $k = a + ib$. The values of k for which there is an attracting orbit are colored gray. The darker the shade of gray, the more critical values are attracted to that orbit.

do not give them here. The most general statement is that scaling the lattice in Proposition 5 by any k of the form $k = \sqrt[3]{e_j/(2mc_j)}$, $j = 1, 2, 3$, $m \in \mathbb{N}$ gives a pole for the critical value e_j.

There is a parameter space for each medium rhombic lattice, since there is a k-space for every value of τ. Small Mandelbrot sets appear, suggesting the existence of attracting periodic orbits and bifurcations, which can be proved in many settings. What seems to be the difference is that the spread of the critical values and critical points prevents toral bands from occurring. In Figure 9 we show a typical parameter space for a medium rhombic lattice of the form $\Lambda = [1, \tau]$, with $\tau = \exp(7\pi i/12)$. We see that the attracting orbits can act independently for the three different critical values. In Figure 10 we see, for the map $\wp(z)$ with $(g_2, g_3) \approx (-2.512, 4.483)]$ that three distinct attracting orbits can occur, one each attracting a critical value. The large discriminants for the lattices and invariants are what causes the spread of the critical values, and this is what changes as we move up along the imaginary axis in the region $\mathfrak{U}$.

References

1. Baker I N, Kotus J, Lü Y (1991) Iterates of meromorphic functions I. Ergodic Theory Dynam. Sys. **11**, 241– 248; and (1991) Iterates of meromorphic functions. III, ETDS **11**, 603 – 618.
2. Baker I N, Kotus J, Lü Y (1992) Iterates of meromorphic functions. IV. Critically finite functions, Results Math. **22**, no. 3-4, 651–656. MR1189754 (94c:58166)
3. Beardon, A (1991) Iteration of rational functions. Complex analytic dynamical systems. Graduate Texts in Mathematics, 132. Springer-Verlag, New York.
4. Bergweiler W (1993) Iteration of meromorphic functions. Bull. Amer. Math. Soc **29**, no. 2: 151 –188.
5. Clemons, J (2012) Connectivity of Julia sets for Weierstrass elliptic functions on square lattices. Proc. Amer. Math. Soc. 140, no. 6, 1963–1972.
6. Devaney R L, Keen L (1988) Dynamics of Tangent, Dynamical Systems, Springer Lecture Notes in Math, #1342, 105-111

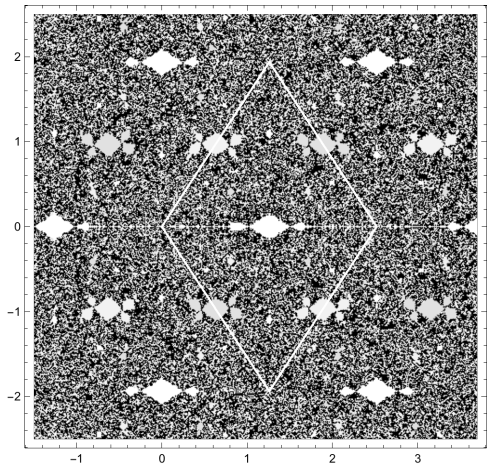

FIGURE 10. We show $J(\wp_\Lambda)$, for $\Lambda = k[1, \tau]$, $\tau = \exp(i\theta)$ a medium rhombic lattice. Points in the Julia set are the darkest. $F(\wp_\Lambda)$ consists of 3 disjoint basins of attraction: one for an attracting real period 4 orbit, and two others for disjoint period 3 attracting orbits, complex conjugates of each other, shown in varying shades of light gray. A fundamental period parallelogram is white.

7. Devaney R L, Keen L (1989) Dynamics of meromorphic maps with polynomial Schwarzian derivative. Ann. Sci. Ecole Norm. Sup. (4), **22**: 55 - 81
8. DuVal P (1973) Elliptic Functions and Elliptic Curves: Cambridge University Press
9. Hawkins, J (2019) Stability of Cantor Julia sets in the space of iterated elliptic functions. Dynamical systems and random processes, 69–95, Contemp. Math., 736, Amer. Math. Soc., [Providence], RI.
10. Hawkins J, Koss L (2002) Ergodic properties and Julia sets of Weierstrass elliptic functions. Monatsh. Math., **137** no. 4: 273 - 300.
11. Hawkins J, Koss L (2004) Parametrized Dynamics of the Weierstrass Elliptic Function, Conf. Geom. Dyn. **8** 1-35.
12. Hawkins J, Koss L (2005) Connectivity Properties of Julia sets of Weierstrass Elliptic Functions, Topology Appl. 152 **no. 1-2**, 107-137.
13. Hawkins J, Koss L (2022) Single and double toral band Fatou components in meromorphic dynamics, preprint.
14. Hawkins J, Moreno Rocha M, (2018) Dynamics and Julia sets of iterated elliptic functions. New York J. Math. 24 , 947 – 979.
15. Hawkins J, Moreno Rocha M, (2021) Unbounded Fatou components for elliptic functions over square lattices, Houston J. Math, 47, 353–374.
16. Jones G, Singerman D (1997) Complex Functions: An algebraic and geometric viewpoint: Cambridge Univ. Press
17. Koss L (2009) A fundamental dichotomy for Julia sets of a family of elliptic functions. Proc. Amer. Math. Soc. 137, 3927-3938.
18. Koss, L (2010) Cantor Julia sets in a family of even elliptic functions, Journal of Difference Equations and Applications 16, 5-6, 675–688.
19. Koss L (2016) Elliptic functions with disconnected Julia sets. Internat. J. Bifur. Chaos Appl. Sci. Engrg. 26, 6, , 53 - 64.
20. Koss L , Roy K (2017) Dynamics of vertical real rhombic Weierstrass elliptic functions. Involve 10 , no. 3, 361 – 378.

21. Kotus J, Urbański, M (2003) Hausdorff dimension and Hausdorff measures of Julia sets of elliptic functions. Bull. London Math. Soc. 35, 2, 269–275.
22. Moreno Rocha, M, (2020) Herman rings of elliptic functions, Arnold Mathematical Journal 6, 551570.
23. Rippon P J, Stallard G (1999) Iteration of a class of hyperbolic meromorphic functions. Proc. Amer. Math. Soc. 127 no. 11, 3251 – 3258.

Department of Mathematics, University of North Carolina at Chapel Hill, CB #3250, Chapel Hill, North Carolina 27599-3250
E-mail address: jmh@math.unc.edu

Department of Mathematics and Computer Science, P.O. Box 1773, Carlisle, PA 17013
E-mail address: koss@dickinson.edu